Solar Photocatalytic Degradation of Textile Dye Direct Blue 86 in ZnO Suspension

by

Syeikh Nuzul Hazwan Bin Yahya

Dissertation submitted in partial fulfillment of
the requirements for the
Bachelor of Engineering (Hons)
(Civil Engineering)

MAY 2013

Universiti Teknologi PETRONAS
Bandar Seri Iskandar
31750 Tronoh
Perak Darul Ridzuan

CERTIFICATION OF APPROVAL

Solar Photocatalytic Degradation of Textile Dye Direct Blue 86 in ZnO Suspension

by

Syeikh Nuzul Hazwan Bin Yahya

A project dissertation submitted to the
Civil Engineering Programme
Universiti Teknologi PETRONAS
in partial fulfillment of the requirement for the
BACHELOR OF ENGINEERING (Hons)
(CIVIL ENGINEERING)

Approved by,

_____
AP DR MOHAMED HASNAIN ISA

UNIVERSITI TEKNOLOGI PETRONAS
TRONOH, PERAK
MAY 2013

CERTIFICATION OF ORIGINALITY

This is to certify that I am responsible for the work submitted in this project, that the original work is my own except as specified in the references and acknowledgements, and that the original work contained herein have not been undertaken or done by unspecified sources or persons.

SYEIKH NUZUL HAZWAN BIN YAHYA

ABSTRACT

Synthetic dyes are found in various products ranging from clothes to leather accessories to furniture. These carcinogenic compounds are the major constituents of industrial wastewater and require removal due to their negative environmental and health effects. This study deals with the photocatalytic degradation of Direct Blue 86 (DB86) by ZnO irradiated using simulated solar light. The effect of initial dye concentration, catalyst loading, irradiation intensity as well as the pH of the dye solution and mineralization of the treated dye were studied. The experiments were carried out by irradiating the aqueous solutions of DB86 containing photocatalyst in a photoreactor. The rate of decolorization was monitored using UV-Vis spectroscopy. The results were modeled based on pseudo first order kinetics. The experimental results indicated that the maximum decolorization of DB86 occurred with 4g/L of ZnO catalyst at pH 10. High irradiation intensities favor photodegradation process while an increase in initial dye concentration reduced the overall photodegradation efficiency. COD reduction up to 84% was achieved under optimized conditions after 40 minutes of irradiation.

ACKNOWLEDGEMENT

First and foremost, I would like to praise Allah SWT for giving me the strength and knowledge to complete this project. My deepest appreciation goes to my FYP supervisors, Prof. Malay Chaudhuri and AP Dr. Mohamed Hasnain Isa, for entrusting me in conducting this project and without their continuous guidance, this project will not be of a success. Special thanks are also extended to Mr. Augustine Chioma Affam for his advice and assistance which has contributed a lot throughout the project duration. Last but not least, I would like to thank all those who had contributed to the success of my work in one way or another including my father, mother and sisters for their support, encouragement and love that gave me the strength to complete my research and thesis.

TABLE OF CONTENTS

LIST OF FIGURES

LIST OF TABLES

CHAPTER 1
INTRODUCTION

1.1 Background of Study

Wastewater from the industry and households has to be treated prior to discharge into water bodies as it contains chemicals and pathogens that pose considerable threats to human livelihoods and the aquatic ecosystem. Most of the main sources of water pollution originate from the unregulated discharge from the industry.

Like most industries, wastewater from textile manufacturing contains high concentration of chemical substances. Dyestuff used to colour fabric is present in high concentrations in wastewater effluent released into the water bodies. A suitable technology is required to treat the discharged wastewater from textile industry as it contains high concentration of dye reagents which is difficult to be treated. There is also a pressing need for dye waste to be sufficiently treated as most modern synthetic dyes are carcinogenic in nature and is relatively stable against the degradation by sunlight (Hamza et al., 1980).

Advanced oxidation processes (AOPs) have been considered as an effective and environmentally sound method for treating textile effluent. One of the most efficient methods in AOPs is the use of semiconductor-based photocatalysis process (Ohtami et al., 2010). In this method, semiconductor is used as catalysts for oxidation process. At present, TiO_2 and ZnO are the commonly-used semiconducting materials for the treatment of pollutants (Evgenidou et al., 2005).

During this process, a small band-gap of energy 3-3.5 eV is provided by the semiconductor with a filled valence band and an empty conduction. As light falls on the surface of the semiconductor, the photon of threshold energy equal to or greater than the energy gap excites an electron from the occupied valence band and promotes it to the unoccupied conduction band, forming excited state conduction band electrons and positive valence band holes. A few processes can be undertaken by these charged

electrons and holes constituting the charge carriers such as: (1) either recombining radiatively or non-radiatively and dispel their input energy as heat, (2) getting trapped onto the surface layer of the catalyst, (3) recombining the trapped charge carriers, and (4) forgoing recombination and reacting with the electron donors or acceptors adsorbed on the surface of the semiconductor activated under the light when recombination (Hagfeldt et al., 1995).

Recent study shows that the photocatalytic behaviour of the semiconductor is largely resulted from the trapped electrons and trapped holes. However, the ultimate quantum efficiency of the photoredox reactions on the semiconductor surface is determined from a competition between all these processes. Besides, the energy band potentials of the semiconductor have to be compatible with that of the redox potentials of the water/hydroxyl radical couple (2.8 eV) (Hoffmann et al., 1995). Several semiconductors have sufficient energies in their band gap to catalyze a wide range of redox reactions. A suitable photocatalyst for pollutant removal should possess a few characteristics such as economically feasible, non-toxic, high photoactivity and high stability in conditions where pollutants are present.

The main advantage of using semiconductor based materials as photoactive catalysts in pollutant removal is the complete conversion of organic compounds into environment friendly substances without creating secondary contaminants (Amrit et al., 2006). It is also easily regenerated and is active under easily obtainable UV-visible photolight. In recent years, ZnO nanopowder has been used as efficient, economic and nontoxic semiconductor photocatalysts for the breakdown of a wide range of organic chemicals and synthetic dyes (Chakrabarti and Dutta, 2004).

1.2 Problem Statement

Improper dye discharge from various industries such as textile, paper, cosmetic and plastics into receiving streams can be one of the sources of water pollution. In the textile industry alone, approximately 280, 000 tons of dye waste is discharged annually worldwide (Jin et al., 2007). Large amount of water is required in the production of fabric, and this causes a high discharge of dye wastewater into the environment.

Prior to its discharge, dye waste poses a considerable hazard to the aquatic ecosystem as it undergoes chemical and biological reaction which subsequently reduces the amount of dissolved oxygen (Huang et al., 2008). As a result, an excessive discharge of dye waste threatens the survival of fishes and other aquatic organisms (Rahman et al., 2009). On top of that, dye compounds do not deteriorate easily and are highly stable against the attack of temperature, light, detergents, chemicals and microbial degradation (Couto, 2009).

Ultimately, the discharge of dye waste into water bodies poses a significant threat to the aquatic ecosystem as it increases the turbidity of water and disrupts the photosynthetic activity of hydrophytes (Aksu et al., 2007), and the presence of toxic compounds due to chemical changes may harm some aquatic organisms (Hao et al., 2000). Besides, most dye compounds are mutagenic and carcinogenic in nature, and the damage may extend from the aquatic ecosystem to human livelihoods.

There are various existing technologies to treat dye waste, namely adsorption process, precipitation, air stripping, flocculation, reverse osmosis and ultra-filtration for removal of dye compounds (Supaka et al., 2004). However, these methods only provide partial treatment by transforming the dye compounds from one form to another without really being disintegrated (Sano et al., 2008), creating secondary pollutions and eventually requires another form of treatment (Slokar and Marechal, 1998).

Thus, a treatment method which is both economical and environment friendly is required for the remediation of dye waste. Photocatalytic oxidation represents an attractive solution for dye waste treatment due to its capacity in oxidizing organic

contaminants to carbon dioxide, water and mineral acids, without creating secondary contaminants.

1.3 Objective and Scope of Study

The principal objective of this study is to investigate the influence of various parameters on photocatalytic degradation of the textile dye Direct Blue 86 (DB86) by ZnO, irradiated using simulated solar light. The effects of key operating parameters such as irradiation intensity, initial concentration of the dye, catalyst loading as well as the pH of the solution on the decolorization of the dye will be studied.

To achieve the objectives, the following scope has been identified:

i. to determine the effect of key operating conditions (catalyst loading, irradiation intensity, pH and initial concentration of the dye) on photocatalytic degradation of Direct Blue 86 and

ii. to determine the mineralization of the treated dye solution (DB86) under optimum operating conditions (catalyst loading and pH of the dye solution).

CHAPTER 2
LITERATURE REVIEW

2.1 Direct Dyes

Direct dyes are the most popular class of dyes due to their easy application, extensive range of colors and low cost. It is also available in powered form which makes it easy to be handled and measured. Another advantage associated with direct dye is it can be applied directly onto textiles without the need of a separate adhesion mechanism. However, there is a common drawback of using direct dyes. Textiles colored using this type of dye tends to 'bleed' or dissipate easily, however there are some treatments that can be done to enhance the permanence of the color onto the fabric. In the Color Index system, direct dye is referred to various planar and highly conjugated molecular structures that contain one or more anionic sulfonate group.

Most direct dyes are azo dyes which are constituted of water-soluble, anionic compounds. The dye compound has a flat shape and a suitable length which enable them to align along-side cellulose fibers and maximize the Van-der-Waals, dipole and hydrogen bonds. Most direct dyes have disazo and trisazo structures. Azo dyes form the largest class (60–70 percent) of dyes with the widest range of colors (Bae and Freeman, 2007).

Due to its wide application, azo dyes are widely dispersed in the aquatic system and possess adverse effects on the aquatic ecosystem. Textile effluent is characterized by high pH, high level of chemical oxygen demand (COD) and biological oxygen demand (BOD) and usually contains a high concentration of chlorides and residual chlorine as well as heavy metal pollutants such as zinc, cadmium, chromium, copper, nickel, lead and mercury (Lanciotti et al., 2004).

Even though textile dyes can be decolorized from anaerobic processes by reducing the azo bond, the aromatic amines produced are more resistant to degradation and may be toxic or genotoxic (Sweeney et al., 1994). Several toxicological studies

have revealed a connection between certain dyes and the incidence of carcinogenic and mutagenic toxicity in organism (Bae et al., 2006; Mathur et al., 2005). Moreover, water bodies which are polluted with water-soluble azo dyes are normally highly colored (Anliker, 1977) and cause aesthetic problems.

2.2 Methods of Dye Removal

Synthetic dye compounds in wastewater cannot be effectively removed using conventional treatment methods due to the properties of recalcitrant organic molecules, its resistance to aerobic degradation and its high stability against sunlight. Another reason is due to the high cost involved in treating dye effluent at large scale in the textile industry (Ghoreishi and Haghighi, 2003). Technologies employed for the removal of dye waste can be divided into three categories i.e. biological, chemical and physical methods (Robinson et al., 2001). There are advantages and drawbacks associated with each treatment method.

2.2.1 Biological Methods

Biological treatment is often the most attractive method in terms of cost-effective as compared with other chemical and physical treatments. Biodegradation methods such as decolourization using fungi, microbial degradation, the use of living or dead microbial biomass in adsorption and bioremediations are commonly applied in the treatment of industrial effluents as a large variety of microorganisms such as bacteria, yeasts, algae and fungi have the capacity to accumulate and degrade different pollutants (Fu and Viraraghavan, 2001; McMullan et al., 2001).

However, the efficiency of biological treatment in dye removal is limited to a certain extent. As stated by Supaka et al. (2004), the use of biological treatment is often constrained by various factors such as the requirement of large land area, low flexibility in design and operation, sensitivity towards diurnal variation and the toxicity of some chemicals. Furthermore, the current biological treatment is also incapable of producing

a satisfactory removal of colour pigments (Robinson et al., 2001). Although some dye components are successfully degraded, many others are recalcitrant due to their complex chemical structure and synthetic organic origin (Kumar et al., 1998). The use of biological treatment is also ineffective in degrading azo dyes due to their xenobiotic nature.

2.2.2 Chemical Methods

Chemical treatments used for wastewater management include coagulation and flocculation combined with flotation and filtration method, precipitation-flocculation process with Fe(II) or $Ca(OH)_2$, electrokinetic coagulation, and electroflotation, conventional oxidation methods by oxidizing agents such as ozone, electrochemical processes and irradiation. These chemical techniques are often costly, and even though the dyes are removed from the wastewater, it is accumulated in the form of concentrated sludge, thus requires another disposal method (Ghoreishi and Haghighi, 2003). There is also a possibility of creating a secondary pollution because of excessive chemical use.

Recently, an emerging technique known as advanced oxidation processes based on the generation of very powerful oxidizing agents such as hydroxyl radicals, have been applied with much success for the pollutant degradation. Although these methods are generally effective for the treatment of waters contaminated with pollutants, it is commercially unattractive due to high cost, high energy consumption and extensive usage of chemicals.

2.2.3 Physical Methods

Various physical treatment methods such as membrane filtration processes and adsorption techniques are also widely used in wastewater management. Membrane filtration includes nanofiltration, reverse osmosis and electrodialysis. The use of membrane filtration processes is mainly restricted by the limited lifetime of membranes

before fouling occurs as well as the cost of periodic replacement that must be included in the analysis of their economic viability.

From the literature, it has been indicated that liquid-phase adsorption is one of the most popular methods for the removal of pollutants from wastewater, as a proper design of an adsorption system is effective in producing a high-quality treated effluent. This process is an attractive alternative for the treatment of wastewater especially if a low-cost sorbent is used and does not require an additional pre-treatment step.

Adsorption is a widely-known equilibrium separation process and has a high efficiency in water decontamination processes (Dabrowski, 2001). The use of adsorption process presents a number of advantages as compared to other techniques such as low initial cost, simplicity and flexibility of design, simple operation, low sensitivity to toxic pollutants and does not result in the formation of harmful substances. There are two mechanisms involved in the process of decolourisation: adsorption and ion exchange processes (Slokar and Marechal, 1998). The mechanism is affected by many physicochemical factors such as dye or sorbent interaction, sorbent surface area, temperature, pH, particle size, and contact time (Kumar et al., 1998). However, it doesn't really degrade the dye.

2.3 Advanced Oxidation Process (AOP)

Advanced Oxidation Processes (AOPs) is defined as a near-ambient temperature and pressure water treatment processes which involves the generation of highly reactive radicals (especially hydroxyl radicals) in a sufficient quantity for effective water purification (Glaze et al., 1987; Maldonado et al., 2007). It has been proved to be one of the most effective treatments for wastewater which are difficult to be treated biologically. By far, this method is successfully used to decompose many toxic and bio-resistant organic pollutants in aqueous solution to acceptable levels without producing additional hazardous by-products or sludge which requires further handling.

These processes are based on the generation of the strongly oxidizing hydroxyl radicals ($OH^{\bullet}$), which oxidize a broad range of organic pollutants present in water and wastewaters (Qamar et al., 2006). Hydroxyl radicals are also characterized by a low selectivity of attack which possesses an attractive feature for an oxidant to be used in wastewater treatment. Many different organic compounds are susceptible to removal or degradation by means of hydroxyl radicals. Once hydroxyl radicals are generated, they can oxidize and mineralize almost every organic molecule, producing CO_2 and inorganic ions.

2.3.1 Basic Principles of Photocatalysis

Photocatalysis is termed as a photoinduced reaction accelerated by the presence of a catalyst. It is activated by the absorption of a photon with sufficient energy, which equals or higher than the band-gap energy of the catalyst. The absorption process leads to a charge separation due to the promotion of an electron (e^{-}) from the valence band of the semiconductor catalyst to the conduction band, thus generating a hole (h^{+}) in the valence band. This process is shown as a schematic diagram in Figure 2.1.

The recombination of the electron and the hole in the valence band must be prevented to favor the photocatalyzed reaction. The purpose of this process is to induce a reaction between the activated electrons with an oxidant to produce a reduced product, as well as a reaction between the generated holes with a reductant in order to produce an oxidized product. Both the oxidation and reduction can take place at the surface of the photoexcited semiconductor photocatalyst (Figure 2.1).

The photogenerated electrons reduces the dye particles or react with electron acceptors such as O_2 molecules adsorbed on the photocatalyst surface or dissolved in water, and reduces it to superoxide radical anion $O_2^{-\bullet}$. In addition, the photogenerated holes can oxidize the organic molecule or react with OH^{-} or H_2O oxidizing them into OH• radicals. With other highly oxidant species such as peroxide radicals, they have been reported to be responsible for the heterogeneous ZnO photodecomposition of organic substrates as dyes. The resulting •OH radical, being a very strong oxidizing

agent (standard redox potential +2.8 V) can oxidize most azo dyes to the mineral end-products.

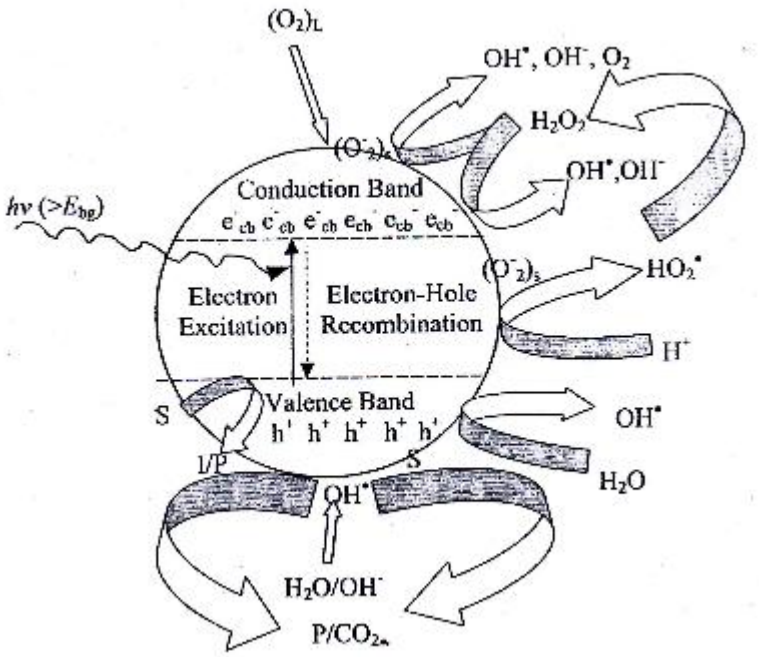

Figure 2.1. Schematic diagram of semiconductor photocatalyst

2.3.2 Mechanisms of ZnO Photocatalysis

The irradiation of ZnO particles with photons of energy equals to or greater than the band gap energy results in the promotion of an electron from the valence band (VB) to the conduction band (CB) of the particle. The outcomes of this process include a region of positive charge known as the "hole" (h^+) in the VB and a free electron (e^-) in the CB.

$$ZnO + hv \rightarrow ZnO\ (e^-_{CB} + h^+_{VB}) \quad (1)$$

The charge carrier species can recombine with the absorbed energy dissipated as heat, or migrates to the particle surface where the holes can react with surface-bound hydroxyl groups (OH^-) and adsorbed water molecules to form hydroxyl radicals ($OH^\bullet$).

$$OH^- + h^+ \rightarrow OH^\bullet \quad (2)$$

$$H_2O + h^+ \rightarrow OH^\bullet + H^+ \quad (3)$$

In the absence of an electron acceptor, the process of electron–hole recombination dominates. The presence of oxygen prevents the recombination process by trapping electrons (through the formation of superoxide ions) and by maintaining electrical neutrality within the ZnO particle. The final product of the reduction is commonly known as hydroxyl radicals ($OH^\bullet$) and hydroperoxyl radical HO_2.

$$2O_2^{\bullet-} + H^+ \rightarrow 2OH + O_2^\bullet \quad (4)$$

$$2O_2^{\bullet-} + H^+ \rightarrow HO_2 \quad (5)$$

Hydroxyl radicals are known to be powerful, indiscriminate oxidizing agents. During the process of photocatalytic reactions, these radicals react with organic compounds which results in degradation.

2.3.3 Effect of pH

The wastewater from textile industries usually has a wide range of pH values. As pH value is also affected by the generation of hydroxyl radicals, it is an important parameter in photocatalytic reactions. In reality, the effect of pH on the efficiency of dye photodegradation process is hard to be determined as there are three possible reaction mechanisms that contribute to the degradation of dye, such as hydroxyl radical

attack (Eq. 6), direct oxidation by the positive hole (Eq. 7) and direct reduction by the electron in the conducting band (Eq. 8) (Faisal et al., 2007).

$$\text{Dye} + OH\bullet \rightarrow \text{degradation product} \quad (6)$$

$$\text{Dye} + h^{+}_{VB} \rightarrow \text{oxidation product} \quad (7)$$

$$\text{Dye} + e^{-}_{CB} \rightarrow \text{reduction product} \quad (8)$$

The efficiency of pH value on photocatalytic degradation must be accurately assessed as pH value varies with the type of dye used, resulting in unique characteristic of textile water. As stated in the literature (Sauer et al., 2002; Neppolian et al., 2002), the value of pH in effluents also affects ZnO activity, including the charge on the particles, the size of the aggregates formed and the positions of the conductance and valence bands. The zero point charge (zpc) for ZnO is 9.0±0.3. ZnO surface is positively charged below pH 9 and will be negatively charged by adsorbed OH^{-} ions above this value. The presence of large quantities of OH^{-} ions on the particle surface as well as in the reaction medium favors the formation of OH• radical, which is widely accepted as principal oxidizing species responsible for decolorization process at neutral or high pH levels and results in enhancement of the efficiency of the process (Akyol et al., 2004).

2.3.4 Effect of Catalyst Loading

From the study conducted by Konstantinou and Albanis (2004) on the review of TiO_2-assisted photocatalytic degradation of azo dyes in aqueous solution, it has been stated that in any reactor system, the initial rates were found to be directly proportional to catalyst concentration which indicate the heterogeneous regime. They have conducted further observation on the limit of catalyst concentration that must be used for the photodegradation of a particular pollutant in wastewater, even to the extent

where the rate of photocatalysis will decrease (Faisal et al., 2007; Rauf et al., 2009). The reason for this is the increase in the amount of catalyst increases the number of active sites available on the photocatalyst surface and results in a higher concentration of hydroxyl and superoxide radicals. However, as the concentration of catalyst has risen above the optimum value, the degradation rate decreases due to the interception of light.

Sun et al. has added that the excessive catalyst which prevents the illumination process results in the reduction of •OH radical, a primary oxidant in the photocatalytic system, and ultimately reduces the efficiency of the degradation process. Furthermore, the increase of catalyst concentration beyond the optimum level may also result in the agglomeration of catalyst particles, preventing the part of the catalyst surface to be unavailable for photon absorption and thus decreases the degradation rate (Faisal et al., 2007).

2.3.5 Effect of Initial Dye Concentration

It is important from both the mechanic and application point of views to study the dependence of the photocatalytic reaction rate on the substrate concentration. It is generally known that the increase in degradation rate is parallel with an increase in dye concentration to a certain level, and a further increase in dye concentration will lead to a decrease in the degradation rate (Saquib and Muneer, 2002). The rate of degradation relates to the formation of •OH radicals on the catalyst surface and to the probability of •OH radicals reacting with dye molecules. There is an increase in the probability of reaction between dye molecules and oxidizing species as the initial concentrations of the dye increase, leading to an enhanced decolorization rate. On the other hand, the degradation efficiency of the dye decreases with a further increase in dye concentration.

The presumed reason is that at a concentration, the generation of •OH radicals on the surface of catalyst will be reduced due to the blocking of active sites by dye ions. Another possible reason for such results is the UV-screening effect of the dye itself. At a high concentration of dye reagents, a significant amount of UV light may be absorbed by the dye molecules rather than the ZnO particles. This results in the reduction of •OH

and $O_2^{\bullet-}$ concentrations and thus decreases the efficiency of the catalytic reaction (Daneshvar et al., 2003). The major portion of degradation process occurs in the region near to the irradiated side (or known as reaction zone) where the irradiation intensity is much higher than on the other side. Therefore at a higher dye concentration, degradation will decrease as the reaction zone moves further away from the light source due to the reduction in light penetration. It can be concluded that as the initial concentration of dye reagent increases, the increase in surface catalyst sites would be required in order to increase the degradation rate (Neppolian et al., 2002).

2.3.6 Effect of Irradiation Intensity and Time

Ollis et al. have provided a comprehensive review of studies reported on the effect of irradiation intensity of photocatalysis kinetics. They had stated that (i) at low irradiation intensities (0–20 mW/cm^2), the rate increases linearly with an increase in irradiation intensity (first order), (ii) reaction rate depends on the square root of the irradiation intensity (half order) at intermediate irradiation intensities beyond a certain value (approximately 25 mW/cm^2), and (iii) at high irradiation intensities, the reaction rate would be independent of irradiation intensity. This is likely because at low irradiation intensity, reactions involving electron–hole formation are predominant and electron–hole recombination is negligible.

On the contrary, at an increased irradiation intensity, there is a competition between electron–hole pair separation and recombination, causing lower effect on the reaction rate. In the previous study (Sauer et al., 2002), the enhancement of decolorization rate due to increased irradiation intensity has also been observed. It is observed that the percentage of decolorization and photodegradation increases with an increase in irradiation time, following the first-order kinetics and additionally a competition for degradation may occur between the reactant and the intermediate products. After a certain time limit, the kinetics of dyes degradation is slowed down due to: (a) the difficulty in the conversion of the N-atoms of dye into oxidized nitrogen compounds, (b) the slow reaction of short chain aliphatics with •OH radicals, and (c) the

short life-time of photocatalyst because of active sites deactivation by strong by-products deposition.

2.4 Kinetics of Photodegradation

The kinetics of the photodegradation of azo dyes is widely mentioned in the literatures. Results from various studies have found to fit the Langmuir-Hinshelwood (L-H) model, where a monolayer of adsorption is occurring on the surface (Konstantinou and Albanis 2004). The L-H model is commonly used to analyze the heterogenous reactions that occur on the surface of catalysts, in which two molecules are required to absorb on the surface for the reaction to occur. Therefore, the concentrations of both species will determine whether reactions take place. Equation (9) shows the rate law which is derived from the model mentioned.

$$r = dC/dt = kKC/(1 + KC) \quad (9)$$

where r is the oxidation rate of the reactant (mg/L min), C the concentration of the reactant (mg/l), t the irradiation time, k the reaction rate constant (min^{-1}), and K is the adsorption coefficient of the reactant (l/mg). At low substrate concentrations, the above equation can be simplified to a pseudo-first order equation (Eq. 10) (Houass et al., 2001).

$$\ln (C_0/C) = kKt = k_{app}t \quad (10)$$

A plot of ln C_0/C versus time represents a straight line, and the slope of which upon linear regression is equivalent to the apparent first-order reaction rate constant. In general, first-order kinetics is relevant for the entire concentration range up to few ppm. The L–H model was derived to describe the dependence of the observed reaction rate on the concentrations of initial solute. Studies have suggested with negligible doubts that the expression for the photomineralization rate of organic substrates such as dyes with

ZnO irradiation conforms with the Langmuir–Hinshelwood (L–H) law in the following four probable circumstances (a) the reaction takes place between two adsorbed substances, (b) the reaction occurs between a radical in solution and an adsorbed substrate molecule, (c) the reaction takes place between a radical linked to the surface and a substrate molecule in solution, and (d) the reaction occurs with the both of species being in solution.

Overall, even though the exact location of the process which takes place either on the surface in the solution or at the interface cannot be identified, the expression for the rate equation is identical to that derived from L–H model and has been successfully-employed in modeling the reaction (Neppolian et al., 2002). Given this, it is likely that the sorption of the dye is an important parameter that determines the rate of photocatalytic degradation. According to the classification stated by Houass et al., all isotherms showed L-shape curves and this shows that there is no strong competition between the water and the dye molecules in occupying the photocatalyst surface sites. Color removal in dye solution is usually determined at the maximum absorption value of every dye by monitoring the UV-Vis spectrum in 200–800 nm zone using a spectrophotometer.

CHAPTER 3

MATERIALS AND METHODS

3.1 Direct Blue 86

Direct Blue (DB86) is the dye investigated in this study. Information on this dye is shown below together with its molecular structure (Figure 3.1).

Name:	Direct Blue 86
Synonyms:	C.I. 74180; Disodium [29H,31H phthalocyaninedisulphonato(4-)-N29,N30,N31,N32]cuprate(2-)

Molecular Structure:

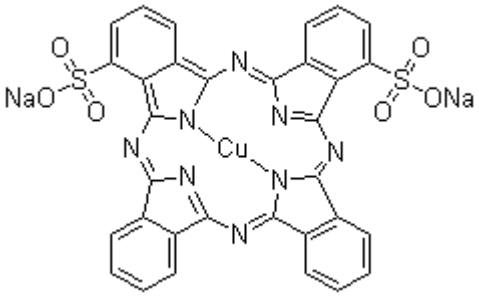

Figure 3.1. Molecular structure of Direct Blue 86

Molecular Formula:	$C_{32}H_{14}CuN_8Na_2O_6S_2$
Molecular Weight:	780.16

Source: http://www.chemblink.com

3.2 Photoreactor

Experiments are carried out in a Solsim photoreactor solar simulator (Figure 3.2). The setup consists of a UV chamber made up of highly reflective aluminum alloy with an internal dimension of 30 cm×30 cm×22 cm and equipped with a 300W xenon lamp fitted on the top of the chamber. To maintain the temperature in the chamber, an exhaust fan was fixed on the backside of the photoreactor.

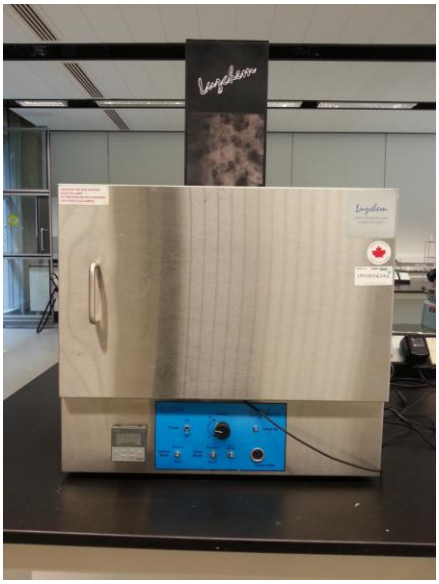

Figure 3.2. Luzchem Solsim solar simulator

3.3 Establishment of Standard Curves of Direct Blue 86 at different pH values

A known concentration of DB86 solution is prepared and wavelength of the maximum absorbance is determined using a spectrophotometer. Different concentrations of DB86 at different pH are prepared from the stock solution and measured for absorbance at the corresponding wavelength of maximum absorbance of the dye in the visible region. The pH level of the solution is adjusted using 1M H_2SO_4 and 1M NaOH. Based on this, a standard curve of absorbance versus concentration of the dye is plotted. This standard curve will be used to measure the concentration of the treated dye solution.

3.4 Photocatalytic Experiment

Batch experiments were performed in a Pyrex reactor (beaker) made of borosilicate glass with a capacity of 250 mL. A fixed amount of DB86 was dissolved in 1000 mL of distilled water and the pH is adjusted using 1M H_2SO_4 and 1M NaOH. The concentration of substrate in the bulk solution at this point was used as the initial concentration (C_0) for kinetic study of the photodegradation process. Except for the

study on effect of irradiation intensity, effects of all the other parameters were studied at irradiation intensity of 300 W/m^2.

Prior to the irradiation process, DB86 solution containing the determined catalyst loading was stirred continuously in the dark for 30 minutes to achieve the adsorption equilibrium of DB86 onto the surface of the catalyst. All irradiation processes were carried out under constant stirring to ensure homogeneity of the suspension. From the intervals of irradiation (t), the solution is withdrawn from the photoreacter and filtered through a Millipore filter (pore size 0.45 µm). The absorbance of the filtrates was analyzed at the maximum absorption wavelength of DB86 (620 nm) using a spectrophotometer. Concentration of the filtrates (C) can be determined from the standard curve of the dye at different pH using the measured absorbance. Graph of ln (C_0/C) against irradiation time (t) was then plotted to obtain the reaction rate constant from the linear slope line of the graph.

The reaction kinetics were studied by varying different parameters of irradiation intensity (300-900 W/m^2), initial pH of the solution (pH 4-10), catalyst loading (1.0-5.5 g/L) and initial concentration of the dye (30-70 mg/L). All the results were modeled and presented based on pseudo first order kinetics. COD analysis of the dye was conducted after the optimum condition has been determined.

3.5 Process Flow Methodology

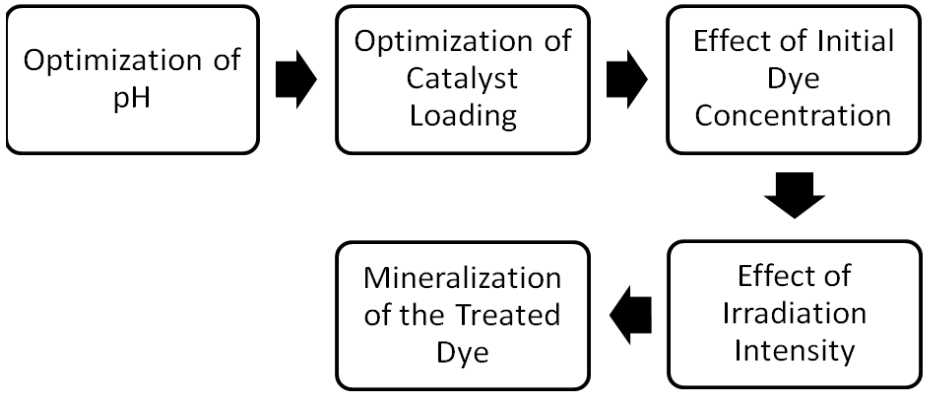

3.6 Apparatus and Materials

The apparatus and materials that are used throughout the experiments are listed below.

3.6.1 Apparatus

- Micropipette
- 200 mL beaker
- 0.45 µm membrane filter
- pH meter
- Magnetic stirrer
- Volumetric flask
- Spectrophotometer
- Test vial
- Solsim photoreactor solar simulator
- COD reactor
- COD vial adapter

3.6.2 Materials

- Direct Blue 86
- Distilled water
- Zinc Oxide, ZnO
- Sulphuric acid, 1M H_2SO_4
- Sodium hydroxide,1M NaOH

3.7 Project Activities and Key Milestones

Table 3.1 below shows the target activities that were already been set for FYP 1 and FYP 2. All the activities have been successfully carried out within the time frame allocated.

Table 3.1. Study plan

Project Activities	FYP I														FYP II													
	1	2	3	4	5	6	7	8	9	10	11	12	13	14	1	2	3	4	5	6	7	8	9	10	11	12	13	14
Background Study																												
Literature Review Reading																												
Extended Proposal Report																												
Preliminary Research Work																												
Establishment of DB86 standard curves at different pH values																												
Design of Experimental Works																												
Extended Proposal Defense																												
Project Work Continues																												
Determination of optimum pH																												
Submission of Interim Draft Report																												
Submission of Interim Report																												
Project Work Continues																												
Determination of optimum catalyst loading																												
Varying initial dye concentration																												
Varying irradiation intensity																												

Study of mineralization of the treated dye solution																													
Discussion and evaluation																													
Pre-SEDEX																													
Submission of Draft Report																													
Submission of Dissertation																													
Submission of Technical Paper																													
Oral Presentation																													
Submission of Final Report																													

Note: ● Key milestones

CHAPTER 4
RESULTS AND DISCUSSION

4.1 UV–visible Spectra of DB86

Figure 4.1 shows the UV–vis spectra measurement of a 50 mg/L DB86 solution at natural pH of 7.10. The absorption peak is observed at 620 nm. The peak gradually decreases as the concentration decreases as the amount of organic compounds is lower for a solution with lower concentration.

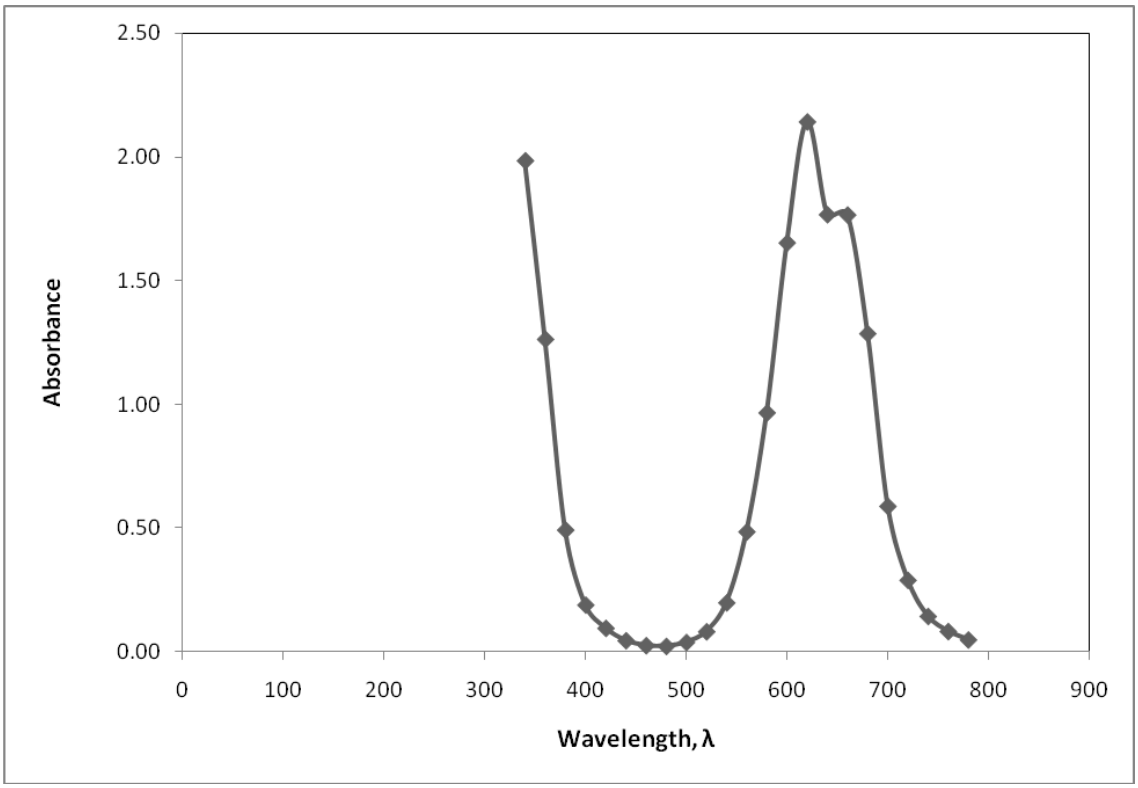

Figure 4.1. Absorption spectrum of DB86 at natural solution pH

4.2 Standard Curves of DB86

Standard curves based on Beer–Lambert's law for DB86 solution at different pH values are plotted by relating the absorbance rate to the concentration of the solution (Figure 4.2). The pH of dye solution is adjusted using 1M H_2SO_4 and 1M NaOH.

Maximum absorption wavelength of DB86 is 620 nm as measured by UV-visible spectrophotometer. A linear relationship between concentration of DB86 and absorbance is induced by varying the initial DB86 dye concentration from 0 mg/L to 100 mg/L at different pH values (Table 4.1). It was then tested with a maximum absorbance at 620 nm. It is important to note that the maximum wavelength and the molar absorption coefficient of DB86 were not significantly dependent on the pH of solution within the range of 3–10. Some deviation could be observed in the calibration curve at pH of 1 and 2 due to the low solubility of dye at this value (Saien and Shahrezaei, 2007).

Table 4.1. Linear relationship between absorbance and concentration of DB86 at different pH values

pH Value	**Linear Relationship between Absorbance and Concentration of DB86**
1	y=0.023x
2	y=0.032x
3	y=0.036x
4	y=0.038x
5	y=0.039x
6	y=0.040x
7	y=0.041x
8	y=0.041x
9	y=0.041x
10	y=0.041x

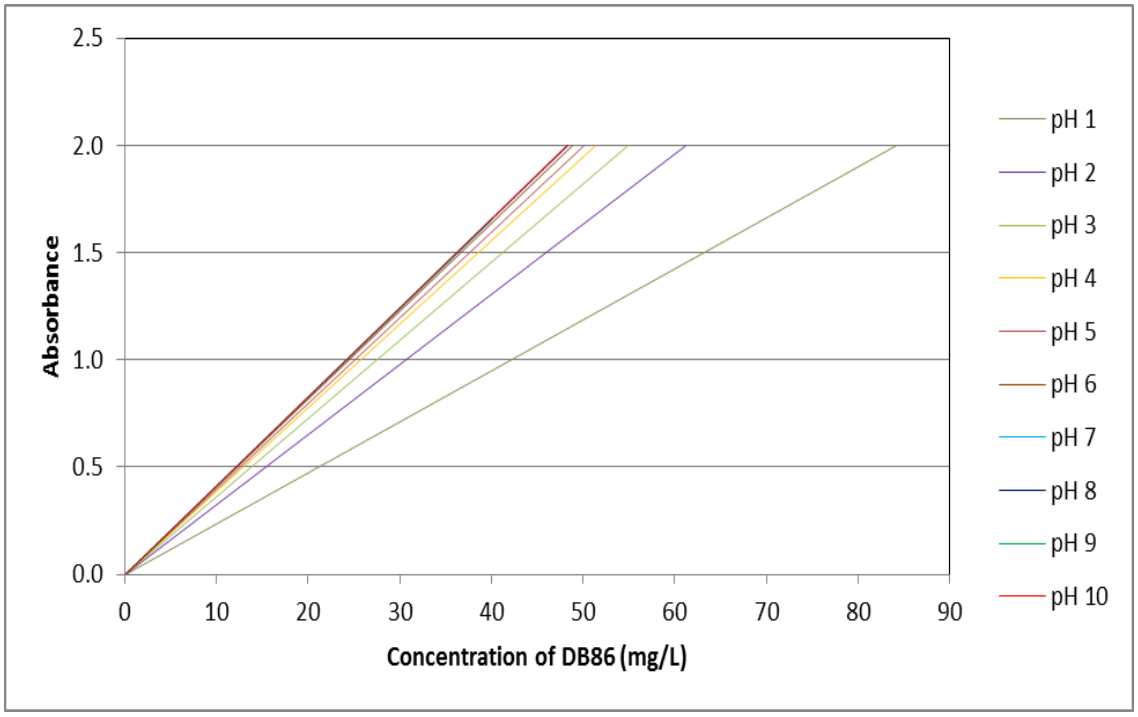

Figure 4.2. Standard curves of DB86 at different pH

4.3 Effect of pH on Photodegradation of DB86

The pH of solution plays an important role in the photocatalytic degradation process of various pollutants. The effect of pH ranging from 4–10 on the photodegradation of DB86 has been studied. The pH of the solution is adjusted before irradiation and it was not controlled during the course of the reaction. The absorbance and respective concentrations of DB86 are listed in Appendix 1. Pseudo first order photodegradation kinetics and reaction rates of DB86 at different ph values together with the correlation coefficient of the straight line have been presented in Figure 4.3, Figure 4.4 and Table 4.2 respectively. After 60 minutes of irradiation, the pseudo-first order rate constants at pH 4, 6, 8 and 10 observed to be 0.0054, 0.0129, 0.0144 and 0.0181 min^{-1}, respectively. The photodegradation is minimal at pH 4 and high in alkaline medium (pH 6-10) where significant removal efficiency of DB86 can be observed. The optimum pH for efficient DB86 removal by ZnO is achieved at pH 10. At an acidic pH range, the removal efficiency is lower due to the dissolution of ZnO (Evgenidou et al., 2005). ZnO can react with acids to produce the corresponding salt at

low acidic pH values. At higher pH value, ZnO surface is negatively charged by adsorbed OH^- ions. The presence of high concentration in OH^- ions on the particle surface as well as in the reaction medium favors the formation of ^-OH radicals in which facilitate the photodegradation reaction (Gonclaves et al., 1999). Thus, initial pH solution of 10 was fixed for further studies (Catalyst loading, initial dye concentration, irradiation intensity and mineralization of the dye).

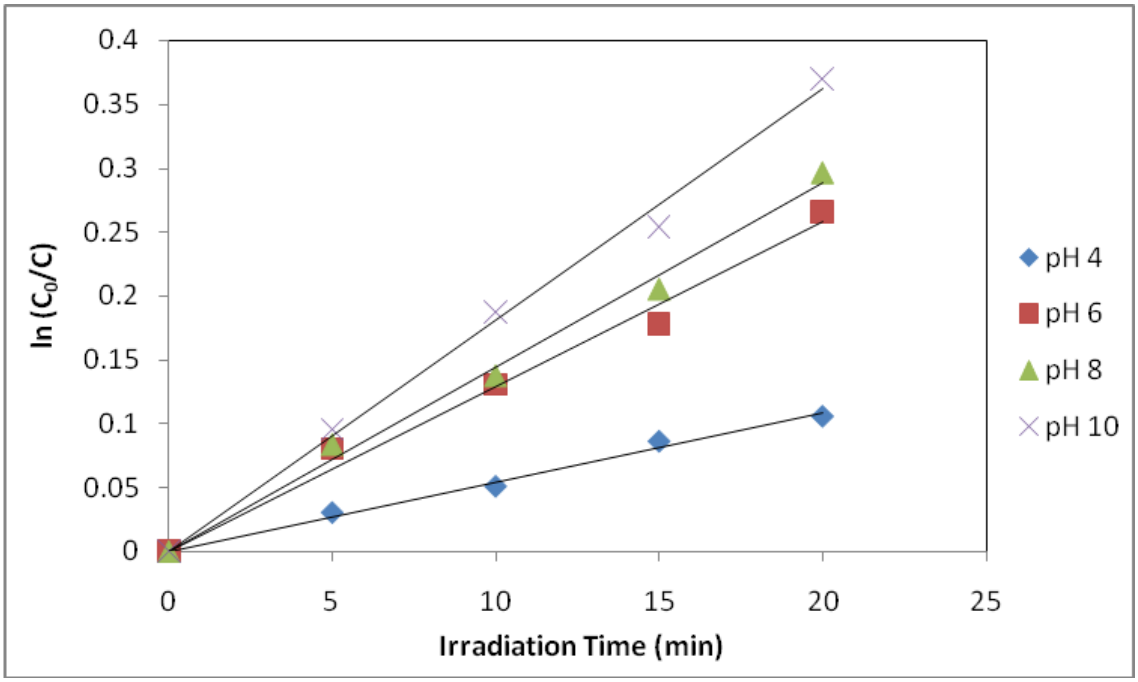

Figure 4.3. Pseudo first order photodegradation kinetics of DB86 at different pH values

Table 4.2. Pseudo first order rate constants at different pH values

pH	Reaction Rate, k (min^{-1})	Correlation Coefficient, R^2
4	0.0054	0.9926
6	0.0129	0.9860
8	0.0144	0.9930
10	0.0181	0.9948

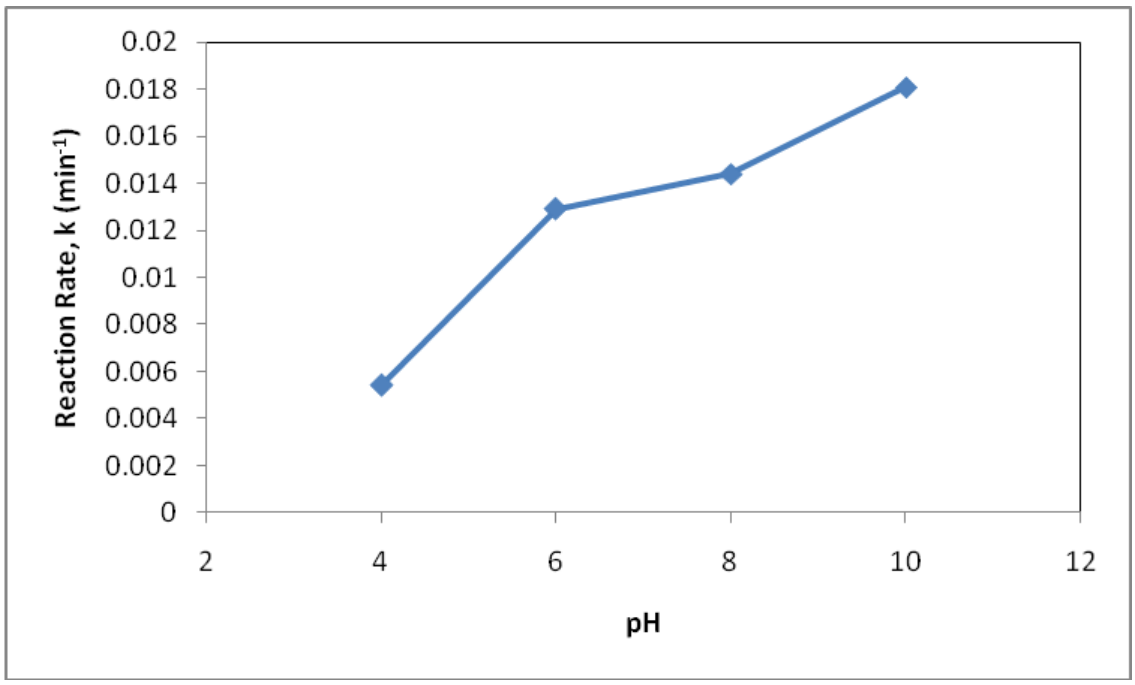

Figure 4.4. Effect of pH on photodegradation of DB86

4.4 Effect of Catalyst Loading on Photodegradation of DB86

To determine the effect of catalyst loading, the concentration of catalyst varying from 1.0 to 5.5 g/L for dye solutions of 50 mg/L at optimum pH 10 is used in the experiment. The absorbance and respective concentrations of DB86 are listed in Appendix 2. Pseudo first order photodegradation kinetics and reaction rates of DB86 at different catalyst loadings together with the correlation coefficient of the straight line have been depicted in Figure 4.5, Figure 4.6 and Table 4.3 respectively. It reveals that the initial reaction rate for the photodegradation process of DB86 increase significantly by increasing the catalyst loading from 1.0 g/L to 4.0 g/L. Maximum decolorization was observed with 4.0 g/L, in which further increase of catalyst concentration decreases the reaction rate of photodegradation. A possible explanation is that optimum catalyst loading is found to be dependent on initial solute concentration. With an increase in the dosage of catalyst, total active surface area increases and more active sites are available on the catalyst surface (Gonclaves et al., 1999). At the same time, due to an increase in the turbidity with high dose of photocatalyst, there will be a decrease in UV light

penetration and this will decrease the photoactivated volume (Daneshvar et al., 2003). It can thus be concluded that higher dosage of catalyst may not be useful in both aggregation and reduced irradiation field due to light scattering. Therefore, catalyst dosage of 4.0 g/L of ZnO in DB86 was fixed for further studies (Initial dye concentration, irradiation intensity and mineralization of the dye).

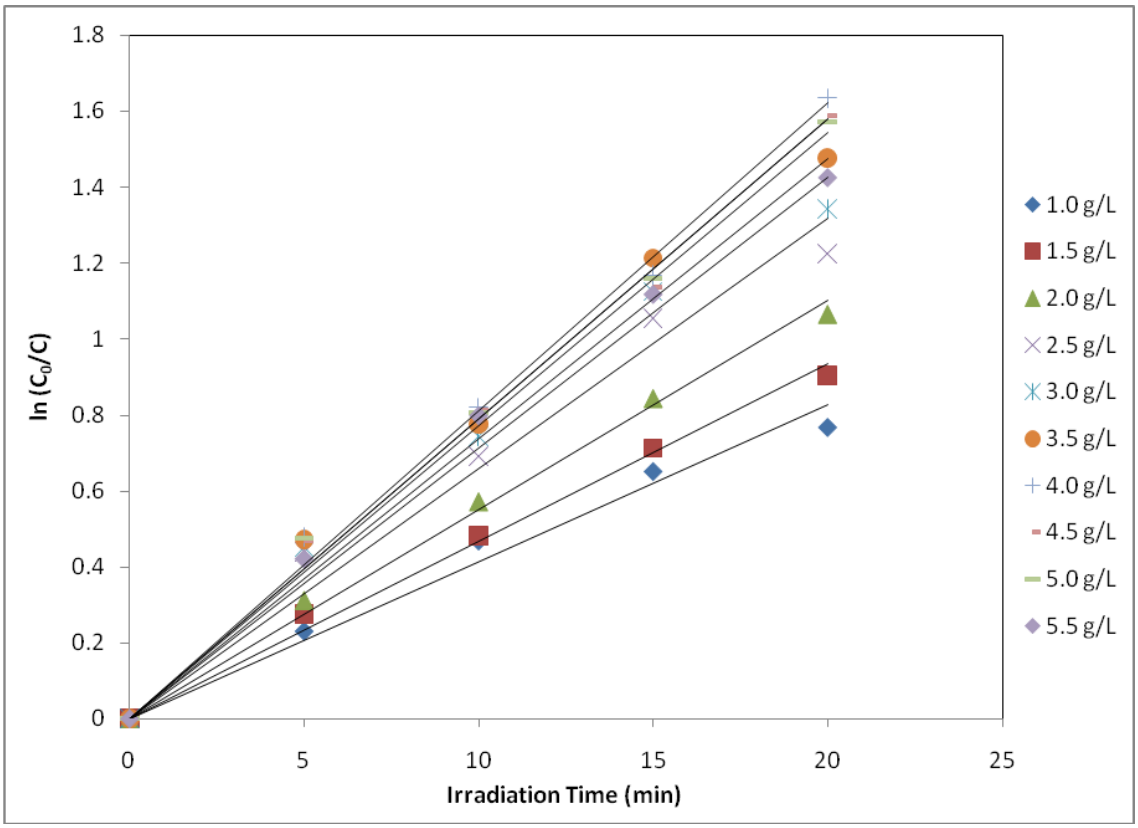

Figure 4.5. Pseudo first order photodegradation kinetics of DB86 at different catalyst loadings

Table 4.3. Pseudo first order rate constants at different catalyst loadings

Catalyst Loading (g/L)	Reaction Rate, k (min^{-1})	Correlation Coefficient, R^2
1.0	0.0413	0.9792
1.5	0.0467	0.9939
2.0	0.0550	0.9953
2.5	0.0659	0.9730

3.0	0.0731	0.9824
3.5	0.0771	0.9893
4.0	0.0811	0.9950
4.5	0.0790	0.9943
5.0	0.0790	0.9950
5.5	0.0738	0.9928

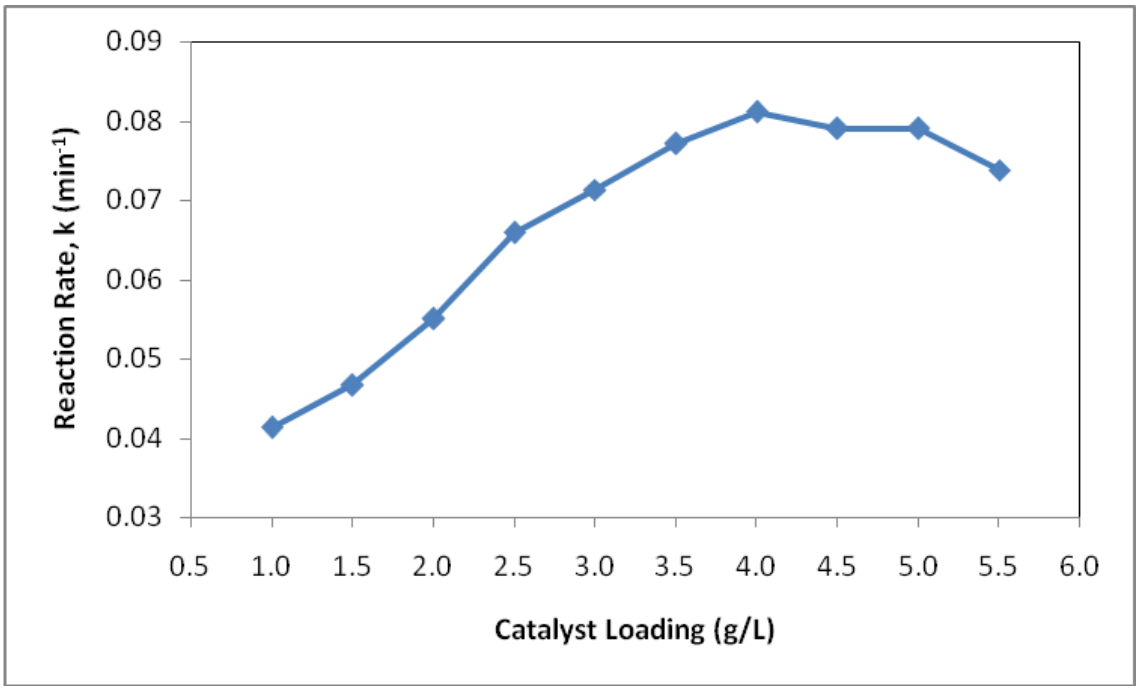

Figure 4.6. Effect of catalyst loading on photodegradation of DB86

4.5 Effect of Initial Dye Concentration on Photodegradation of DB86

After optimizing the pH and concentration of the catalyst, the photocatalytic decolorization of the dye was carried out by varying the initial concentrations of dye from 30 to 70 mg/L in order to assess its effect on the photodegradation process of DB86. The absorbance and respective concentrations of DB86 are listed in Appendix 3. Pseudo first order photodegradation kinetics and reaction rates of DB86 at different initial dye concentration together with the correlation coefficient of the straight line

have been shown in Figure 4.7, Figure 4.8 and Table 4.4 respectively. As the concentration of the dye increased, the rate of photodegradation decreased, which indicates the need for dose of catalyst to be increased or time span for the complete removal to be prolonged. An explanation to this behavior is that as initial concentration increases, more and more organic substances are adsorbed on the surface of ZnO, therefore the generation of hydroxyl radicals will be reduced since there are only a fewer active sites for adsorption of hydroxyl ions and generation of hydroxyl radicals. Furthermore, as the concentration of a dye solution increases, the photons are intercepted before they can reach the catalyst surface resulted in low absorption of photons by the catalyst, which then contributed to lower photodegradation efficiency (Daneshvar et al., 2003). A reverse effect can be observed in a low concentration of the dye. Consequently, in a lower concentration, the number of photon absorption could be increased by increasing the dosage of catalyst (Neppolian et al., 2002).

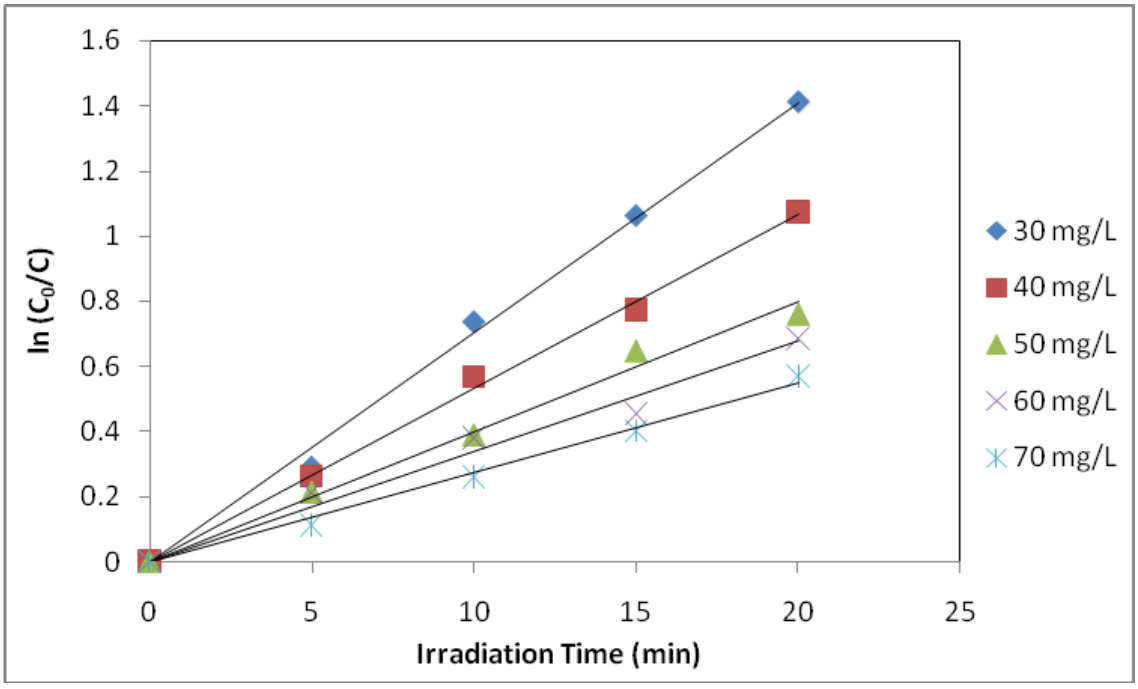

Figure 4.7. Pseudo first order photodegradation kinetics of DB86 at different initial dye concentrations

Table 4.4. Pseudo first order rate constants at different initial dye concentrations

Initial Dye Concentration (mg/L)	Reaction Rate, k (min^{-1})	R^2
30	0.0705	0.9962
40	0.0535	0.9974
50	0.0399	0.9897
60	0.0339	0.9756
70	0.0275	0.9931

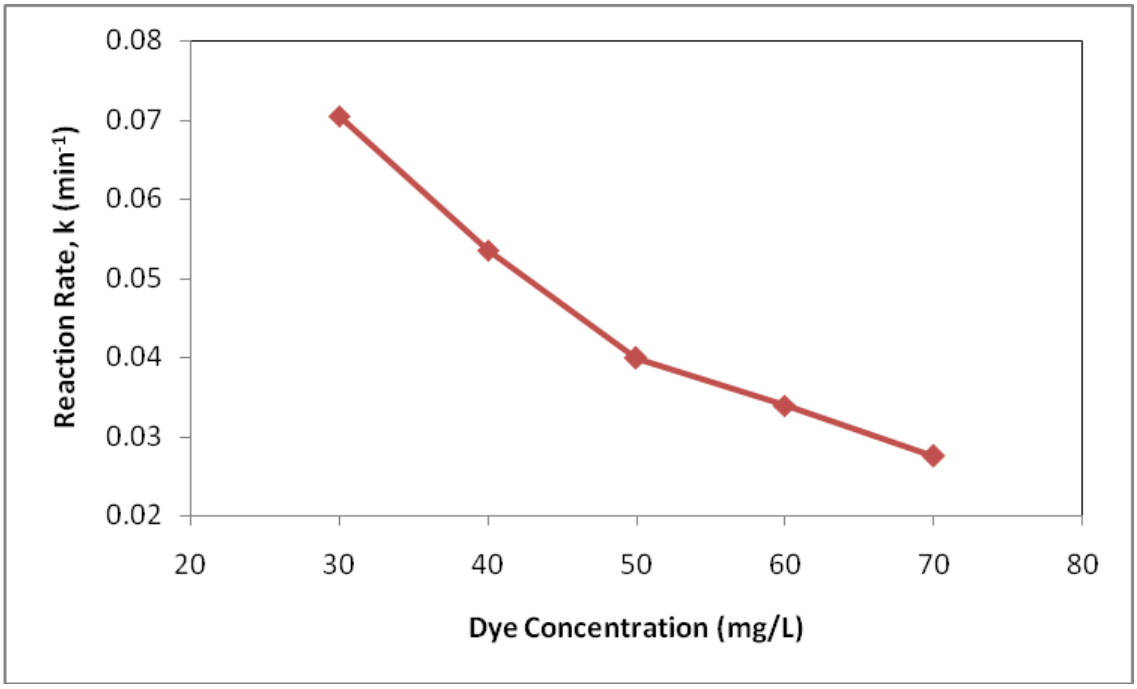

Figure 4.8. Effect of initial dye concentration on photodegradation of DB86

4.6 Effect of Irradiation Intensity on Photodegradation of DB86

The influence of irradiation intensity on the photodegradation process was studied by varying the irradiation intensity from 300 W/m^2 to 900 W/m^2 at constant dye concentration of 50 mg/L and catalyst loading of 4g/L. The absorbance and respective concentrations of DB86 are listed in Appendix 4. Pseudo first order photodegradation kinetics and reaction rates of DB86 at different irradiation intensities together with the

correlation coefficient of the straight line have been depicted in Figure 4.9, Figure 4.10 and Table 4.5 respectively. It is evident that the reaction rate of photodegradation increases with increasing the light intensity. UV irradiation generates the photons required for the electron transfer from the valence band to the conduction band of a semiconductor photocatalyst, hence the overall energy input to a photocatalytic process is dependent on the irradiation intensity. The rate of degradation increases when more radiations fall on the catalyst surface and hence more hydroxyl radicals are produced increasing the overall photodegradation efficiency (Amrit et al., 2006).

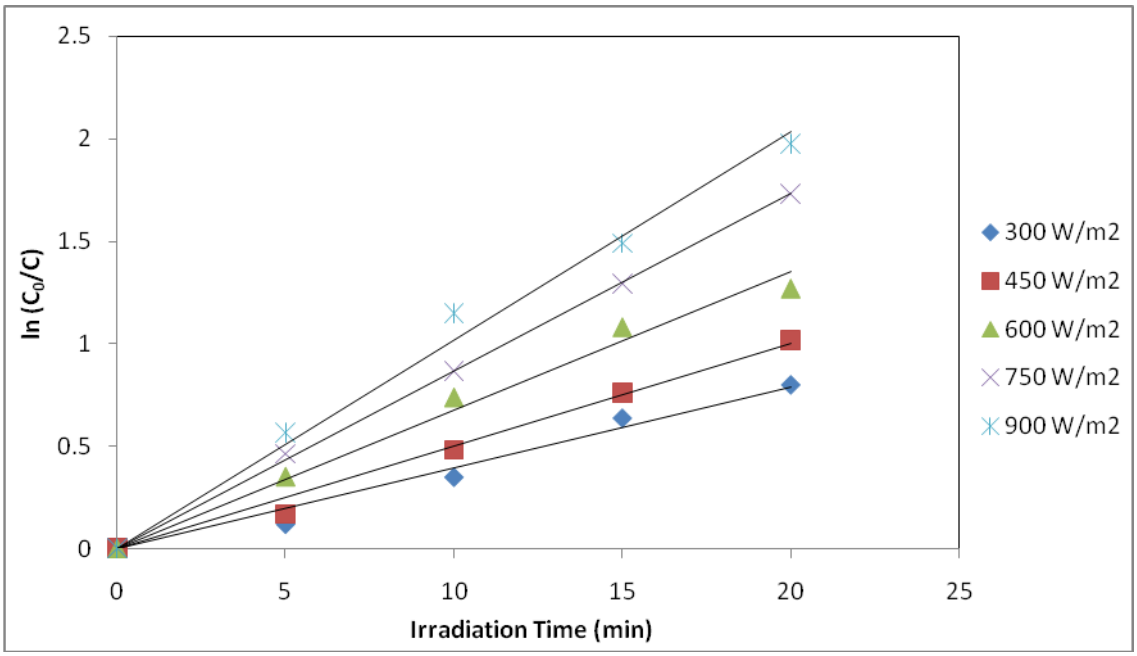

Figure 4.9. Pseudo first order photodegradation kinetics of DB86 at different irradiation intensities

Table 4.5. Pseudo first order rate constants at different irradiation intensities

Irradiation Intensity (W/m^2)	**Reaction Rate, k (min^{-1})**	**Correlation Coefficient, R^2**
300	0.0394	0.9769
450	0.0500	0.9891
600	0.0676	0.9858

750	0.0867	0.9995
900	0.1017	0.9895

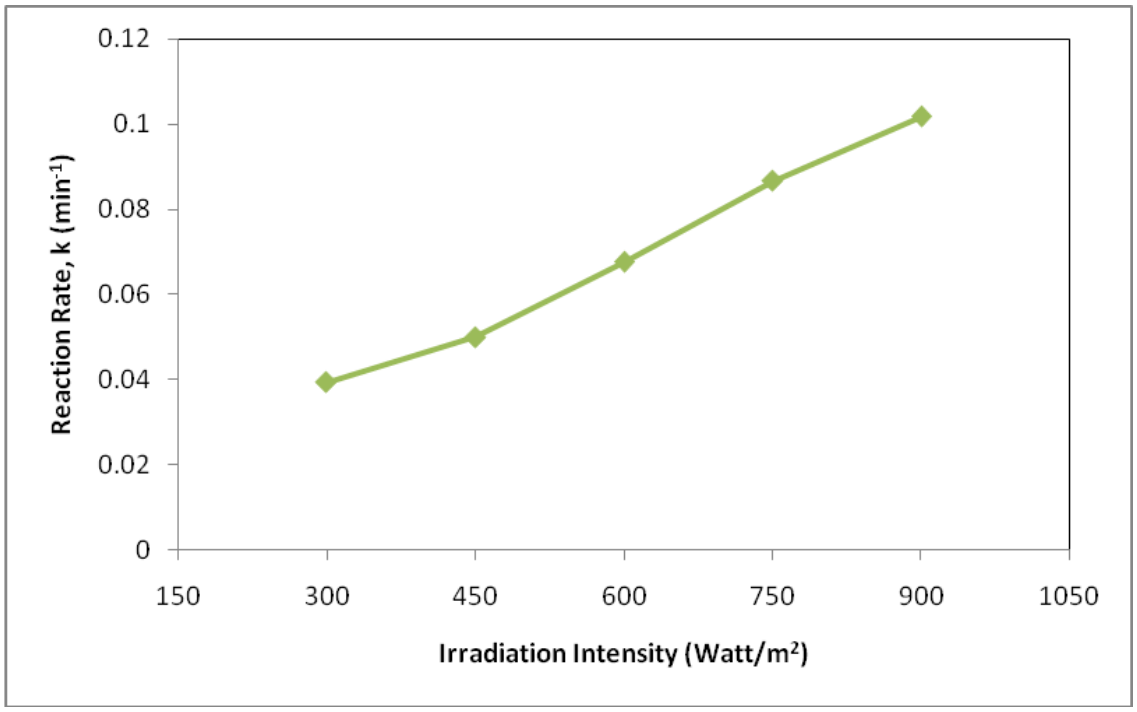

Figure 4.10. Effect of irradiation intensity on photodegradation of DB86

4.7 Mineralization of the Treated Dye under Optimum Operating Condition

As a reduction in chemical oxygen demand (COD) reflects the extent of degradation or mineralization of organic species, the change in COD values of DB86 was studied under optimized condition as a function of irradiation time with initial dye concentration of 50mg/L and irradiation intensity of 850 W/m^2. Overview of the photodegradation process of DB86 under optimized condition is shown in Table 4.6 and Figure 4.11. It can be observed that total discoloration of the dye can be achieved at irradiation time of 40 minutes and reduction of COD up to 84%.

Samples of COD are taken at an interval of 10 minutes and the results are shown in Table 4.7 and plotted in Figure 4.12. It can be observed that during the early stages of the photodegradation process, only a small decrease of COD is measured. This is due to

the fact that when the solution is still coloured, the dye molecules are first decomposed to lower molecular weight compounds and the resulting intermediates still contribute to the COD of the solution. After the decolorization of the solution, COD value decreases sharply indicating that almost complete mineralization of intermediates has occurred (Konstantinou and Albanis, 2004). The COD reduction is less than the percentage of decolorization which may be due to the formation of smaller uncolored products (Kansal et al., (2007). Therefore, it seems that in order to achieve complete mineralization of the dye, a longer irradiation time is required.

Table 4.6. Concentration of DB86 at different irradiation times

Parameter	**Irradiation Time (min)**				
	0	**10**	**20**	**30**	**40**
Concentration of DB86	50	22.3	9.3	1.3	0

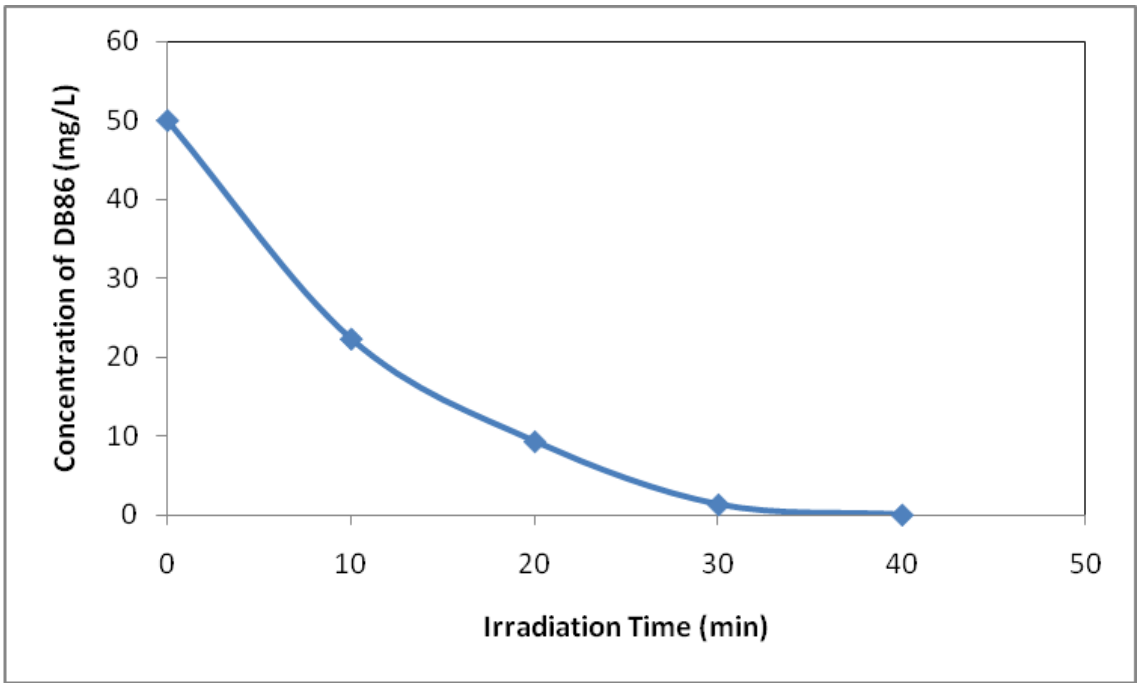

Figure 4.11. Photodegradation of DB86 under optimized condition

Table 4.7. COD value at different irradiation times

Parameter	Irradiation Time (min)				
	0	**10**	**20**	**30**	**40**
COD (mg/L)	25	22	18	11	4

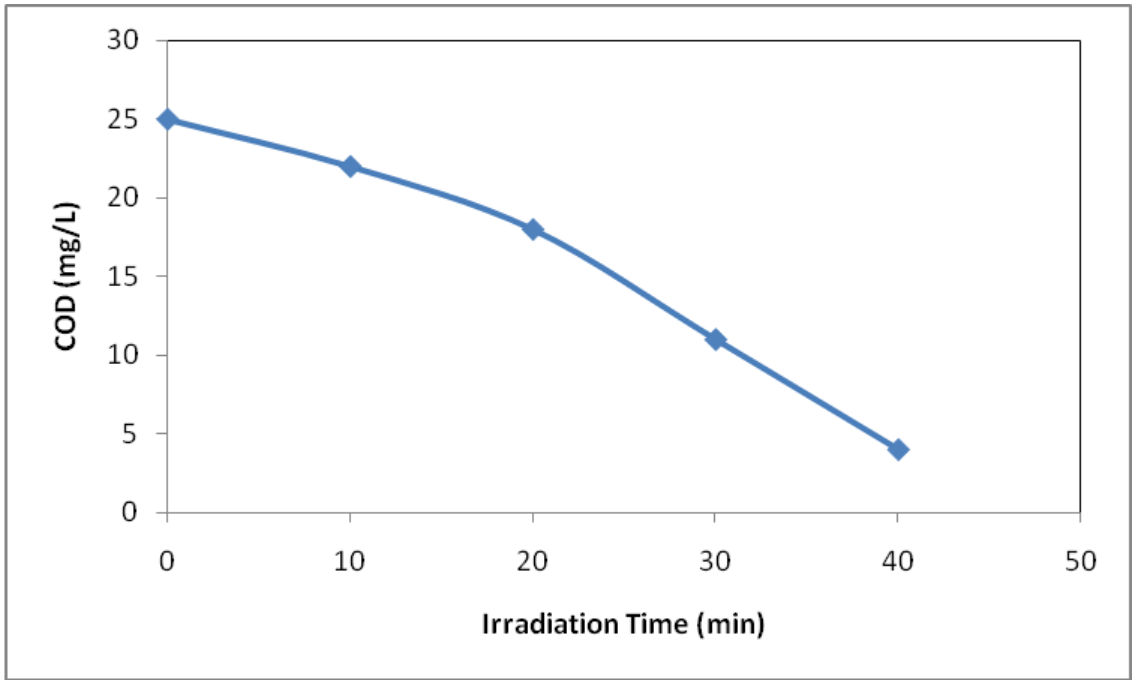

Figure 4.12. Mineralization (COD) of DB86 under optimized condition

CHAPTER 5
CONCLUSION AND RECOMMENDATION

5.1 Conclusion

Effective photocatalytic degradation of Direct Blue 86 (DB86) is possible by employing heterogeneous photocatalytic process using ZnO suspension. The experimental results indicated that the degree of photodegradation was significantly affected by irradiation intensity, initial concentration of the dye, catalyst loading as well as the initial pH of the solution. It is observed that photodegradation of DB86 was most efficient in solution of pH 10 with 4g/L of photocatalyst. The photodegradation efficiency is enhanced with the increase of irradiation intensity whereas reverse effect is obtained with the increase of initial dye concentration. Complete removal of color, after selection of optimal operational parameters could be achieved in a relatively short time of 40 minutes irradiation time and COD removal of 84% was achieved under the optimized condition. In conclusion, this study has demonstrated that photocatalysis is a very effective technology for degrading textile dye.

5.2 Recommendations

Characterization of the photocatalyst in terms of X-ray diffraction (XRD), scanning electron microscope (SEM) and specific surface area (BET) should be conducted to study the morphology and other characteristics of the photocatalyst used in the photodegradation process. Fourier transform infrared (FTIR) spectrum of the untreated and treated dye samples should also be analyzed to assess the chemical bonds and molecular structure of the dye before and after the treatment process. Moreover, toxicity tests of the treated dye waste will gather useful information about the practical application of the photocatalytic process. Overall, better understanding of the photocatalytic process and the operative conditions could give great opportunities for its application for the destruction of environmental organic contaminants in the future.

REFERENCES

Aksu, Z., Kilic, N.K., Ertugrul, S. and Donmez, G., 2007, "Inhibitory effects of chromium(VI) and remazol black B on chromium(VI) and dyestuff removals by Trametes versicolor," *Enzyme and Microbial Technology* 40: 1167-1174.

Akyol, A., Yatmaz, H.C. and Bayramoglu, M., 2004, "Photocatalyticdecolorization of Remazol Red RR in aqueous ZnO suspensions," *Applied Catalysis B: Environmental* 54: 19.

Amrit P.T., Anoop, V., Jotshi, C.K., Bajpai, P.K. and Vasundhara, S., 2006, "Photocatalytic degradation of direct yellow 12 dye using UV/TiO_2 in a shallow pond slurry reactor," *Dyes and Pigments* 68: 53-60.

Anliker, R., 1977, "Colour chemistry and the environment," *Ecotoxicology and Environmental Safety* 1: 211-237.

Bae, J.S. and Freeman, H.S., 2007, "Aquatic toxicity evaluation of new direct dyes to the Daphnia magna," *Dyes and Pigments* 73: 81-85.

Bae, J.S., Freeman, H.S. and Kim, S.D., 2006, "Influence of new azo dyes to the aquatic ecosystem," *Fibers and Polymers* 7: 30-35.

Chakrabarti, S. and Dutta, B.K., 2004, "Photocatalytic degradation of model textile dyes in wastewater using ZnO as semiconductor catalyst," *Journal of Hazardous Materials* 112: 269-278.

Couto, S.R., 2009, "Dye removal by immobilised fungi," *Biotechnology Advances* 27: 227-235.

Dabrowski, A., 2001, "Adsorption – from theory to practice," *Advances in Colloid and Interface Science* 93: 135-224.

Daneshvar, N., Salari, D. and Khataee, A.R., 2003, "Photocatalytic degradation of azo dye acid red 14 in water on ZnO as an alternative catalyst to TiO_2," *Journal of Photochemistry and Photobiology A: Chemistry* 157: 111.

Evgenidou, E., Fytianos, K. and Poulios, I., 2005, "Semiconductor-sensitized photodegradation of dichlorvos in water using TiO_2 and ZnO as catalysts," *Applied Catalysis B: Environmental* 59: 81-89.

Faisal, M., Abu Tariq, M. and Muneer, M., 2007, "Photocatalysed degradation of two selected dyes in UV-irradiated aqueous suspensions of titania," *Dyes and Pigments* 72: 233-239.

Fu, Y. and Viraraghavan, T., 2001, "Fungal decolorization of dye wastewaters: a review," *Bioresource Technology* 79: 251-262.

Ghoreishi, M. and Haghighi, R., 2003, "Chemical catalytic reaction and biological oxidation for treatment of non-biodegradable textile effluent," *Chemical Engineering Journal* 95: 163-169.

Glaze, W.H., Kwang, J.W. and Chapin, D.H., 1987, "Chemistry of water treatment processes involving ozone, hydrogen peroxide and ultraviolet radiation," *Ozone Science and Engineering* 9: 335-352.

Gonclaves, M.S.T., Oliveira, A.M.F., Pinto, E.M.M.S., Plasencia, P.M.S. and Queiroz, M.J.R.P., 1999, "Photochemical treatment of solutions of azo dyes containing TiO_2," *Chemosphere* 39: 781.

Hagfeldt, A. and Gratzel, M., 1995, "Light-induced redox reactions in nanocrystalline systems," *Chemical Reviews* 95: 49-68.

Hamza, A. and Hamoda, M.F., 1980, Proc. 35th Purdue industrial waste congress, West Lafayette, USA.

Hao, O.J., Kim, H. and Chaing, P.C., 2000, "Decolorization of wastewater," *Critical Reviews in Environmental Science and Technology* 30: 49-505.

Hoffmann, M.R., Martin, S.T., Choi, W. and Bahnemann, D., 1995, "Environmental applications of semiconductor photocatalysis," *Chemical Review* 95: 69-96.

Houass, A., Lachheb, H., Ksibi, M., Elaloui E. and Guillard, C., 2001, "Photocatalytic degradation pathway of methylene blue in water," *Applied Catalysis B: Environmental* 31: 145-157.

Huang, M., Xu, C., Wu, Z., Huang, Y., Lin, J. and Wu, J., 2008, "Photocatalytic discolorization of methyl orange solution by Pt modified TiO_2 loaded on natural zeolite," *Dyes and Pigments* 77: 327-334.

Jin, X., Liu, G., Xu, Z. and Yao, W., 2007, "Decolorization of a dye industry effluent by Aspergillus fumigatus XC6," *Applied Microbiology and Biotechnology* 74: 239-243.

Kansal, S.K., Singh, M. and Sud, D., 2007, "Studies on photodegradation of two commercial dyes in aqueous phase using different photocatalysts," *Journal of Hazardous Materials* 141: 581-590.

Konstantinou, I.K.. and Albanis, T.A., 2004, "TiO_2-assisted photocatalytic degradation of azo dyes in aqueous solution: kinetic and mechanistic investigations - A review," *Applied Catalysis B: Environmental* 49: 1-14.

Kumar, V., Wati, L., Nigam, P., Banat, I.M., Yadav, B.S., Singh, D. and Marchant, R., 1998, "Decolorization and biodegradation of anaerobically digested sugarcane molasses spent wash effluent from biomethanation plants by white-rot fungi," *Process Biochemistry* 33: 83-88.

Lanciotti, E., Galli, S., Limberti, A. and Givannelli, L., 2004, "Ecotoxicological evaluation of wastewater treatment plant effluent discharge: a case study in Parto (Tuscany, Italy)," *Annali di Igiene* 16: 549-558.

Maldonado, M.I., Passarinho P.C. and Oller, I., 2007, "Photocatalytic degradation of EU priority substances: a comparison between TiO_2 and fenton plus photo-fenton in a solar pilot plant," *Journal of Photochemistry and Photobiology A* 185(2-3): 354-363.

Mathur, N., Bhatnagar, P., Nagar, P. and Bijarnia, P.K., 2005, "Mutagenicity assessment of effluents from textile dye industries of Sanganer, Jaipur (India): a case study," *Ecotoxicology and Environmental Safety* 61: 105-113.

McMullan, G., Meehan, C., Conneely, A., Kirby, N., Robinson, T., Nigam, P., Banat, I. M., Marchant, R. and Smyth, W.F., 2001, "Microbial decolourisation and degradation of textiles dyes," *Application Microbial Biotechnology* 56: 81-87.

Neppolian, B., Shankar, M.V. and Murugesan, V., 2002, "Semiconductor assisted photodegradation of textile dye," *Journal of Scientific and Industrial Research* 61: 224-230.

Ohtami, B., 2010, "Photocatalysis- A to Z – What we know and what we do not know in a scientific sense," *Journal of Photochemistry and Photobiology C: Photochemistry Reviews* 11(4): 157-178.

Ollis, D.F., Pelizzetti, E, and Serpone N., 1991, "Destruction of water contaminants," *Environmental Science and Technology* 25:1523.

Qamar, M., Muneer, M. and Bahnemann, D., 2006, "Heterogeneous photocatalysed degradation of two selected pesticide derivatives, triclopyr and daminozid in aqueous suspensions of titanium dioxide," *Journal of Environmental Management* 80: 99-106.

Rahman, M.M., Hasnat, M.A. and Kazuaki, S., 2009, "Degradation of commercial textile dye by fenton's reagent under xenon beam irradiation in aqueous medium," *Journal of Scientometric Research* 1: 108-120.

Rauf, M.A. and Ashraf, S.S., 2009, "Application of advanced oxidation processes (AOP) to dye degradation – an overview," *Dyes and Pigments*: New Research, Nova Science Publishers, Inc., Hauppauge.

Robinson, T., McMullan, G., Marchant, R. and Nigam, P., 2001, "Remediation of dyes in textiles effluent: a critical review on current treatment technologies with a proposed alternative," *Bioresource Technology* 77: 247-255.

Saein, J. and Shahrezaei, F., 2007, "Decolorization and mineralization of direct blue86 by UV/TiO_2 process: Investigations on the effect of operational parameters," *Journal of Sciences Islamic Azad University* 17: 64.

Sano, T., Puzenat, E., Guillard, C., Geantet, C. and Matsuzawa, S., 2008, "Degradation of C_2H_2 with modified-TiO_2 photocatalysts under visible light irradiation," *Journal of Molecular Catalysis* A: Chemical 284: 127-133.

Saquib, M. and Muneer ,M., 2002, "Semiconductor mediated photocatalysed degradation of anthraquinone dye, remazol brilliant blue R under sunlight and artificial light source," *Dyes and Pigments* 53:237.

Sauer, T., Neto, G.C., Jose, H.J. and Moreira, R.F.P.M., 2002, "Kinetics of photocatalytic degradation of reactive dyes in a TiO_2 slurry reactor," *Journal of Photochemistry and Photobiology A* 149: 147-154.

Slokar, Y.M. and Marechal, A.M.L., 1998, "Methods of decoloration of textile wastewaters," *Dyes and Pigments* 37: 335-356.

Sun, J., Qiao, L., Sun, S. and Wang, G., 2008, "Photocatalytic degradation of Orange G on nitrogen-doped TiO_2 catalysts under visible light and sunlight irradiation," *Journal of Hazardous Materials* 155: 312-319.

Supaka, N., Juntongijin, K., Damronglerd, S., Delia, M.L. and Strehaiano, P., 2004, "Microbial decolorization of reactive azo dyes in a sequential anaerobic–aerobic system," *Chemical Engineering Journal* 99: 169-176.

Sweeney, E.A., Chipman, J.K. and Forsythe, S.J., 1994, "Evidence for direct-acting oxidative genotoxicity by reduction products of azo dyes," *Environmental Health Perspectives* 102: 119-122.

APPENDIX 1

Effect of pH on Photodegradation of DB86

Table 1. Absorbance of DB86

pH	Irradiation Time (min)				
	0	**5**	**10**	**15**	**20**
4	2.030	1.969	1.929	1.862	1.826
6	2.030	1.873	1.781	1.699	1.556
8	2.030	1.867	1.769	1.653	1.509
10	2.030	1.845	1.683	1.574	1.402

Table 2. Concentration of DB86

pH	Irradiation Time (min)				
	0	**5**	**10**	**15**	**20**
4	49.51	48.02	47.05	45.41	44.54
6	49.51	45.68	43.44	41.44	37.95
8	49.51	45.54	43.15	40.32	36.80
10	49.51	45.00	41.05	38.39	34.20

APPENDIX 2

Effect of Catalyst Loading on Photodegradation of DB86

Table 1. Absorbance of DB86

Catalyst Loading (g/L)	Irradiation Time (min)				
	0	5	10	15	20
1.0	2.045	1.624	1.280	1.066	0.949
1.5	2.045	1.551	1.262	1.002	0.827
2.0	2.045	1.497	1.154	0.879	0.704
2.5	2.045	1.319	1.024	0.712	0.600
3.0	2.045	1.300	0.971	0.663	0.533
3.5	2.045	1.277	0.941	0.608	0.467
4.0	2.045	1.268	0.901	0.636	0.399
4.5	2.045	1.280	0.908	0.657	0.418
5.0	2.045	1.273	0.913	0.642	0.425
5.5	2.045	1.342	0.921	0.669	0.492

Table 2. Concentration of DB86

Catalyst Loading (g/L)	Irradiation Time (min)				
	0	5	10	15	20
1.0	49.88	39.61	31.22	26.00	23.15
1.5	49.88	37.83	30.78	24.44	20.17
2.0	49.88	36.51	28.15	21.44	17.17
2.5	49.88	32.17	24.98	17.37	14.64
3.0	49.88	31.71	23.68	16.17	13.00
3.5	49.88	31.15	22.95	14.83	11.39
4.0	49.88	30.93	21.98	15.51	9.73
4.5	49.88	31.22	22.15	16.02	10.20
5.0	49.88	31.05	22.27	15.66	10.37
5.5	49.88	32.73	22.46	16.32	12.00

APPENDIX 3

Effect of Initial Dye Concentration on Photodegradation of DB86

Table 1. Absorbance of DB86

Dye Concentration (mg/L)	**Irradiation Time (min)**				
	0	**5**	**10**	**15**	**20**
30	1.245	0.932	0.597	0.431	0.304
40	1.664	1.280	0.944	0.767	0.568
50	1.998	1.613	1.353	1.046	0.933
60	2.458	1.991	1.679	1.561	1.237
70	2.824	2.522	2.179	1.890	1.595

Table 2. Concentration of DB86

Dye Concentration (mg/L)	**Irradiation Time (min)**				
	0	**5**	**10**	**15**	**20**
30	30.37	22.73	14.56	10.51	7.41
40	40.59	31.22	23.02	18.71	13.85
50	48.73	39.34	33.00	25.51	22.76
60	59.95	48.56	40.95	38.07	30.17
70	68.88	61.51	53.15	46.10	38.90

APPENDIX 4

Effect of Irradiation Intensity on Photodegradation of DB86

Table 1. Absorbance of DB86

Irradiation Intensity (W/m^2)	Irradiation Time (min)				
	0	**5**	**10**	**15**	**20**
300	2.026	1.801	1.432	1.074	0.913
450	2.026	1.713	1.252	0.947	0.73
600	2.026	1.427	0.969	0.688	0.57
750	2.026	1.275	0.852	0.557	0.358
900	2.026	1.149	0.642	0.456	0.28

Table 2. Concentration of DB86

Irradiation Intensity (W/m^2)	Irradiation Time (min)				
	0	**5**	**10**	**15**	**20**
300	49.41	43.93	34.93	26.20	22.27
450	49.41	41.78	30.54	23.10	17.80
600	49.41	34.80	23.63	16.78	13.90
750	49.41	31.10	20.78	13.59	8.73
900	49.41	28.02	15.66	11.12	6.83